



Contents lists available at SciVerse ScienceDirect

Earth and Planetary Science Letters

journal homepage: www.elsevier.com/locate/epsl

Extractable organic material in fault zones as a tool to investigate frictional stress

Pratigya J. Polissar^{a,*}, Heather M. Savage^{b,1}, Emily E. Brodsky^{c,2}^a Lamont-Doherty Earth Observatory of Columbia University, Division of Biology and Paleo Environment, 61 Rt. 9W, Palisades, NY 10964, United States^b Lamont-Doherty Earth Observatory of Columbia University, Division of Seismology, Geology and Tectonophysics, 61 Rt. 9W, Palisades, NY 10964, United States^c Department of Earth and Planetary Sciences, University of California, Santa Cruz, 1156 High St., Santa Cruz, CA 95060, United States

ARTICLE INFO

Article history:

Received 2 March 2011

Received in revised form 16 August 2011

Accepted 2 September 2011

Available online xxxx

Edited by: L. Stixrude

Keywords:

frictional heat

extractable organic matter

thermal maturity

Punchbowl Fault

Kodiak Accretionary Complex

ABSTRACT

The detection of a frictional heating signature is an attractive, but elusive, way to measure frictional stress on exhumed faults with no evidence of melting. We present a new paleothermometer for fault zones that utilizes the thermal maturity of extractable organic material to determine the maximum frictional heating experienced by the fault. Because there are no retrograde reactions in these organic systems, maximum heating is preserved. We investigate the Punchbowl Fault, an ancient strand of the San Andreas Fault in southern California. According to the methylphenanthrene index for thermal maturity, there is no differential heating between the fault and off-fault samples, indicating that the fault did not get hotter than the surrounding rock during slip. Additionally, the thermal maturity of the rocks falls within the range of heating expected from the bounds on burial depth and time, and adds some constraint to the burial depth range. Simple heating models indicate that the fault must have had either 1) an extremely low shear stress during slip, 2) an active slipping zone thicker than 1 mm, or 3) earthquakes smaller than ~M6, to lack a differential heating signature after 44 km slip.

© 2011 Elsevier B.V. All rights reserved.

1. Introduction

Determining the absolute stress on faults during slip is one of the major goals of earthquake physics as this information is necessary for full mechanical modeling of the rupture process. One indicator of absolute stress is the total energy dissipated as heat through frictional resistance. The heat results in a temperature rise on the fault that is potentially measurable and interpretable as an indicator of the absolute stress.

Despite the relatively straightforward theoretical effect, fault heating has been difficult to constrain in nature. Early work attempted to capture the total integrated dissipated energy over geological time by measuring modern heat flow in boreholes in the vicinity of the San Andreas Fault (Brune et al., 1969; Lachenbruch and Sass, 1980; 1992). Those studies failed to find an increase in temperature over the San Andreas. This negative result can be interpreted as evidence of very low resisting stress (less than 20 MPa shear stress resolved along the fault). However, metrics that are sensitive to integrated energy sources are also sensitive to integrated energy sinks. In this case, heat can be removed by fluid circulation between slip events and requires significant hydrological modeling to interpret (Fulton et al., 2010). Another strategy is to measure the temperature of a fault immediately after a large earthquake (Kano et al., 2006; Tanaka et al., 2001), however,

no project to date has succeeded in drilling fast and deep enough with sufficient repeated measurements to unequivocally capture the transient heating signature. Still another strategy is to examine geological indicators, like pseudotachylyte, fission tracks or vitrinite reflectance, to reconstruct ancient heating (d'Alessio et al., 2003; O'Hara, 2004; Rowe et al., 2005). Although promising, these indicators are somewhat rare (pseudotachylyte; see Kirkpatrick et al., 2009, for further discussion), can be easily reset by temperature fluxes (fission track) or may be influenced by shear strain (vitrinite).

Here we take an alternative strategy to determining the temperature rise on an exhumed fault by using the thermal alteration of organic molecules. Heating organic matter leads to systematic changes in its structure, bulk composition and molecular geochemistry. These changes are routinely used in the petroleum industry to evaluate the thermal history of petroleum source rocks and crude oils. The thermal maturity of organic matter reflects the integrated time–temperature history of a rock. However, the chemical kinetics that govern thermal maturation are strongly temperature dependent and the reactions are irreversible, making it extremely sensitive to peak temperature.

We measured the molecular composition of organic matter to determine the thermal maturity near a well-studied fault zone, the Punchbowl Fault of Southern California. As this is a new application of these organic geochemical measurements, we first offer a brief discussion of the methodology before presenting the key results that show no differential heating on the Punchbowl Fault and potentially no heating in excess of that expected from burial. Based upon models for frictional heating on faults, this result constrains either the resolved shear stress to be low during slip, the thickness of the fault

* Corresponding author. Tel.: +1 845 365 8400(office); fax: +1 845 365 8150.

E-mail addresses: polissar@ldeo.columbia.edu (P.J. Polissar),hsavage@ldeo.columbia.edu (H.M. Savage), brodsky@es.ucsc.edu (E.E. Brodsky).¹ Tel.: +1 845 365 8720(office).² Tel.: +1 831 459 1854(office).

zone to be much larger than suggested based upon field observations or the maximum size earthquake to be small. After discussing the Punchbowl Fault, we present some of the limitations of the technique as illustrated by measurements on small faults in the Monterey Formation, California. Finally, we discuss some more enigmatic results from the Kodiak Accretionary Complex, Alaska.

2. Background

Organic matter in sediments is made up of insoluble material (kerogen) and soluble material (bitumen). When organic matter is buried and heated, several processes occur including generation of new bitumen from kerogen, destruction of bitumen and rearrangement of molecular structures to more stable configurations. All of these processes allow us to track the thermal maturity of organic material. Here, we are looking at the changes in the molecular composition of bitumen with heating (often termed biomarker analysis). Alternative methods currently in use measure the thermal maturity of the kerogen (i.e. vitrinite reflectance). Temperature and time both contribute to organic metamorphism by providing the energy for the reactions to proceed (temperature) and determining the reaction extent (time). These reactions are irreversible, therefore organic maturity is particularly sensitive to the maximum temperature during heating.

Organic maturation occurs over a wide range of time and length scales and has been used to investigate many geologic processes. Vitrinite reflectance and molecular parameters are used to measure thermal maturation due to burial (e.g. Beaumont et al., 1985; Mukoyoshi et al., 2006; O'Hara et al., 1990; Underwood et al., 1988). In addition, both molecular parameters and vitrinite have been used on shorter time scale phenomena such as igneous intrusions, wildfires, lightning strikes (Daly et al., 1993; Farrimond et al., 1999; Raymond and Murchison, 1992; Schimmelmalm et al., 2009; Simoneit, 2002) and rapid shock heating of high-velocity projectiles and targets (Bowden et al., 2008, 2009; Parnell et al., 2010).

In recent years, vitrinite reflectance has been increasingly utilized to detect thermal signatures in faults. Progressive heating of vitrinite increases its reflectance in the visible spectrum, which can be measured with a microscope and has been extensively calibrated to time–temperature heating histories in nature and the laboratory (c.f. Burnham and Sweeney, 1989; Sweeney and Burnham, 1990). Positive vitrinite anomalies have been measured in the Lewis Thrust (Montana), Spring Mt. Thrust (Kentucky), South Wales Coalfield, Gellihorn nappe (Switzerland), Chelungpu Fault (Taiwan), and the Megasplay Fault currently being drilled in the Nankai Accretionary Complex (Bustin, 1983; O'Hara, 2004; Sakaguchi et al., 2007, 2011; Suchy et al., 1997). High-speed rotary friction experiments have also revealed changes in vitrinite reflectance in frictionally heated coal gouge samples (O'Hara et al., 2006).

A molecular approach provides new information on fault heating. It is applicable to rock types where vitrinite is sparse or absent (e.g. marine organic matter) and can be measured on fault gouge where comminution may yield vitrinite particles too small to measure (e.g. Rowe, 2007). In addition, molecular parameters could be used to evaluate the effects of shearing on vitrinite reflectance. A number of studies suggest that deformation may have a catalytic effect on the maturation of vitrinite. In laboratory experiments, shearing increased vitrinite reflectance as well as decreased the activation energy for conversion of vitrinite to graphite in coal (Mastalerz et al., 1993; Ross and Bustin, 1990; Wilks et al., 1993). These observations suggest that deformation may play a role in determining vitrinite reflectance in fault zones independent of heating.

An extensive variety of molecular biomarker parameters are used to determine thermal maturity and each operates over different time–temperature ranges (Fig. 1) (Peters et al., 2004). These parameters can be analyzed on small samples in many different types of sedimentary environments. Marine, lacustrine and terrestrial organic matter

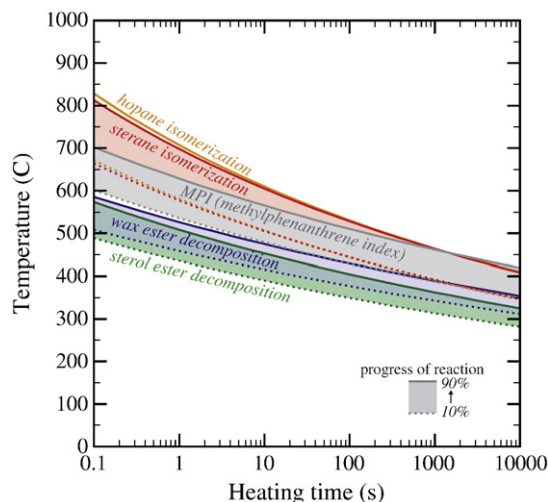


Fig. 1. Progress of different biomarker reactions as a function of time and temperature. The width of each color swath represents where the reaction has progressed between 10% and 90% of the total (kinetic parameters from: Alexander et al., 1992, 1997; Burnham and Sweeney, 1989; Elie and Mazurek, 2008; Mackenzie and McKenzie, 1983; Marzi et al., 1990; Sweeney and Burnham, 1990). The methylphenanthrene index (MPI) progress was calculated from modeling of vitrinite reflectance (R_0) and the empirical relationship between MPI and R_0 from studies of sedimentary basin heating.

contribute molecules that can be used to measure thermal maturity, thus molecular biomarker maturity can be applied to most sediment types. At low maturities, sterane and hopane isomerization indices are often used to evaluate thermal history (Mackenzie and McKenzie, 1983). These indices track the conversion and increasing abundance of thermodynamically favored molecular arrangements relative to the original, less stable, biological arrangements. Another example, useful at higher temperatures, is the preference for methyl branches on polycyclic aromatic compounds to occupy low-steric strain positions on the molecule with increasing maturity (Radke, 1988). At still higher temperatures the relative abundance of diamondoid hydrocarbons increases during the destruction of bitumen (thermal cracking of petroleum) (Wei et al., 2006). These examples illustrate the types of molecular measurements that can be used to assess thermal maturity. The strength of a molecular approach is that a large number of different, independent measurements can be used to determine the thermal alteration of each sample (Fig. 1) and constrain the time–temperature history.

In this paper, we use the methylphenanthrene index (MPI) because these compounds are present in our samples. The MPI is correlated to vitrinite reflectance, as the kinetics of MPI maturation have not been determined. This correlation is based upon measurements of methylphenanthrenes and vitrinite in basin sediments where thermal maturation is due to burial heating. However, this correlation may underestimate heating at fast rates because organic maturation is best described by multiple reaction pathway kinetics that are sensitive to heating rate (Burnham and Braun, 1998). By using this correlation we assume that methylphenanthrenes have kinetics identical to vitrinite even at fast heating rates. While these kinetics have not been tested at fast heating rates, this correlation is sufficient to illustrate the utility of our approach and, as we discuss below, provides a minimum estimate for the amount of rapid heating that may have occurred.

The laboratory and geologic calibrations of biomarker and vitrinite have been conducted at timescales of minutes to millions of years. As fault heating occurs at shorter timescales (seconds to minutes) it is important to know whether biomarker and vitrinite maturation reactions can also occur during fault slip. There is evidence from a number of

geologic and laboratory studies that rapid heating of organic matter is sufficient to increase the thermal maturity. For example, laboratory studies of hypervelocity impacts demonstrate that thermal maturation of methylphenanthrenes, hopanes and other biomarkers can occur in tens of milliseconds at high temperature (Bowden et al., 2008). Furthermore, experiments on the pyrolytic decomposition of methylphenanthrenes indicate there is a time/temperature limit above which methylphenanthrenes will effectively be destroyed (Behar et al., 1999). Extrapolation of the decomposition kinetics from the experimental conditions (1–216 h and 400–452 °C) to shorter timescales indicates almost 100% loss of 9-methylphenanthrene heated at 800 °C for 1.5 s. Additional examples where short heating times cause chemical changes in organic matter include the synthesis of fullerenes in soils during lightning strikes (Daly et al., 1993) and the production of polycyclic aromatic hydrocarbon during combustion of biomass and fossil fuels (e.g. Simoneit, 2002).

Although there is evidence that organic maturation occurs at short timescales, studies show that MPI ratios may not mature as quickly as vitrinite at short timescales. For example, two studies of thermal maturation adjacent to igneous dyke intrusions found that methylphenanthrene ratios increased less than predicted (Bishop and Abbott, 1995; Raymond and Murchison, 1992). These studies indicate that any differential heating signature detected with the MPI ratio likely provides a minimum estimate. In sum these data indicate that short duration, high-temperature heating during earthquake slip should leave a measurable signature in the organic biomarker composition but that the magnitude of heating may be underestimated by kinetic models based upon burial heating rates.

2.1. Temperature sensitivity

In this study, we analyzed a suite of different biomarkers including methylphenanthrenes and other polycyclic hydrocarbons, steranes and hopanes. We focused on methylphenanthrenes because these molecules have not reached their maximum thermal maturity values in the fault rocks discussed here. Furthermore, methylphenanthrenes (unlike other polycyclic hydrocarbons) have been calibrated to vitrinite reflectance. The rate of vitrinite maturation can be described by first-order Arrhenius kinetics on a set of parallel reactions that describe the complex chemistry occurring during maturation (Burnham and Sweeney, 1989; Sweeney and Burnham, 1990):

$$dw_i/dt = -w_i A \exp(-E_i/RT(t)) \quad (1)$$

where w_i is the amount of unreacted component i , A is the pre-exponential factor (identical for all components), E_i is the activation energy of the i th component, R is the universal gas constant and T is temperature which can be a function of time. Note that Eq. (1) results in extreme sensitivity to the peak temperature at short timescales. Over the relatively small time window at which fault heating occurs (milliseconds to tens of seconds) the reasonable range of possible heating temperatures has a much larger effect than the range of heating times. Thus, the peak temperature is the dominant control on reaction kinetics for fault heating timescales. In particular, the integral of Eq. (1) is:

$$\ln w_i = \int_{\tilde{t}=0}^{\tilde{t}} A \exp(-E_i/RT(\tilde{t})) d\tilde{t} \quad (2)$$

The extent of reaction F is:

$$F = 1 - \sum_{i=1}^n f_i (w_i/w_{i,0}) \quad (3)$$

where f_i is the stoichiometric coefficient for the i th parallel reaction component and $w_{i,0}$ is the initial amount of the i th component. These equations are integrated over a prescribed time–temperature

history to calculate the extent of reaction F which is exponentially related to the vitrinite reflectance (R_0) empirically by (Sweeney and Burnham, 1990):

$$R_0 = e^{(-1.6+3.7F)} \quad (4)$$

Combining Eqs. (2)–(4) helps illustrate the sensitivities of the metric:

$$R_0 = e^{2.1 \prod_{i=1}^n e^{-f_i e^{A_i t e^{-E_i/RT}}} \quad (5)$$

For an isothermal history, Eq. (5) illustrates that R_0 is a highly non-linear function of heating duration and peak temperature. Short exposure to higher temperatures – such as during fault slip – has a large effect on vitrinite reflectance and R_0 is most sensitive to the total time spent near the peak temperature. Therefore, in the absence of any additional processes, vitrinite reflectance records the total time at a high temperature regardless of whether that time occurs contiguously or in a series of separate events. This last aspect will be particularly important for drawing conclusions from the fault rocks.

3. Principal site and methods

3.1. Punchbowl Fault

The Punchbowl Fault is an ancient strand of the San Andreas system that has been exhumed from depths of approximately 2–4 km and was active for approximately 1–4 My (Chester and Chester, 1998; Chester and Logan, 1986; Chester et al., 1993; Schulz and Evans, 2000; Wilson et al., 2003). The nearly vertical strike-slip fault juxtaposes sedimentary rocks of the Miocene–Pliocene Punchbowl Formation against basement gneisses and schists. The reason for choosing the Punchbowl Fault for our study was that, in some outcrops, the fault is extremely localized, with a fault core approximately 4–10 cm in width. Certain outcrops also contain a very thin layer (~1 mm) that may have hosted a few kilometers of displacement (Chester and Chester, 1998). Because thinner faults will have a greater temperature rise per unit of heating, the chance of capturing a heating signature along thin fault zones is maximized. The samples in this study were collected from the South Fork area of the fault (Fig. 2) (Dor et al., 2006). We sampled the fault core and damage zone in the Punchbowl Formation and the basement rocks for approximately 100 m along strike.

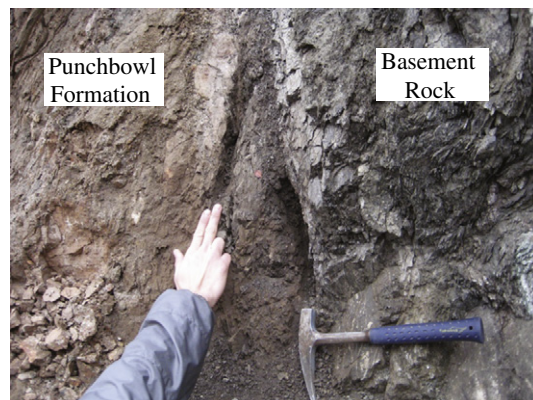


Fig. 2. Outcrop of one of the sampling sites along the Punchbowl Fault.

3.2. Laboratory analyses

We examined a suite of potential markers all of which are well-studied and calibrated for petroleum applications (sterane and hopane isomerization, methylphenanthrenes, Peters et al., 2004) (Fig. 1). Steranes originate from eukaryotic organisms (plants, algae), hopanes from prokaryotic organisms (bacteria) and methylphenanthrenes from cyclic terpenoid precursors derived from plants, algae and bacteria. Samples were physically and chemically cleaned prior to crushing and extraction. The surfaces of samples were first scraped clean and then the rock was broken into 1–2 cm³ pieces. These pieces were visually examined for mineral precipitates and chemical alteration (which were removed). Pieces were then soaked in dichloromethane for 20–60 min to remove any surface contamination (from fracture surfaces and from handling the sample). Samples were crushed with either a silicon carbide shatterbox or agate mortar and pestle that were cleaned with soap and water followed by rinsing with de-ionized water, methanol, dichloromethane and hexane. Following the dichloromethane rinse, all sample handling and storage was with either solvent-rinsed tools or glassware ashed at 450 °C for 8 h. Blanks from the crushing procedure did not yield detectable amounts of any of the compounds we analyzed.

The soluble organic matter was extracted from crushed samples with dichloromethane. Several grams of organic rich sediment were extracted while up to 100 g were extracted of the coarse-grained low-organic rocks of the Punchbowl formation. A few of the samples were extracted with a Soxhlet apparatus using pre-extracted cellulose thimbles while the majority were extracted with a Dionex accelerated solvent extractor (ASE). ASE samples were extracted at 100 °C and 1000 psi for 15 min with 3 static cycles and 90% flush volume and the solvent removed with a dry N₂ stream in a Turbovap evaporator. Soxhlet samples were refluxed for 24 h, the solvent removed by rotary evaporation and then processed in the same way as the ASE samples. Total extracts were separated into aliphatic, aromatic and polar fractions with silica gel column chromatography. Silica gel columns were prepared in Pasteur pipettes with 0.5 g pre-extracted silica gel activated at 200 °C for 2 h. Samples were dissolved in 200 µl of hexane and loaded onto the column. The aliphatic, aromatic and polar fractions were eluted with 2.0 ml hexane (aliphatic), 1.5 ml 7:3 hexane:DCM (aromatic) and 0.5 ml of DCM followed by 1.5 ml of methanol (polar). With this elution scheme, polycyclic aromatic compounds eluted in the aromatic fraction but small quantities of monoaromatic compounds were found in the aliphatic fraction.

The aliphatic and aromatic fractions were analyzed by gas chromatography (GC) with both a flame ionization detector (FID) and mass spectrometer detector (MSD). GC–FID analyses used an Agilent 6890 GC–FID with on-column injection, 60 m DB-5 column (0.25 mm i.d., 0.1 µm film thickness) and H₂ as the carrier gas. During injection the oven was held at 60 °C and then heated at 15 °C/min to 170, 2 °C/min to 280 °C and 15 °C/min to 320. GC–MS analyses used an Agilent 6890 GC with 5970 MSD, split/splitless injector operated in pulsed splitless mode, 30 m DB-5 column (0.25 mm i.d., 0.25 µm phase thickness), He carrier (1.5 ml/min) and MSD at 240 °C with an electron energy of 70 eV. The injector was held at 300 °C and the oven at 60 °C during injection with a 1.5 min hold and then temperature programming identical to the GC–FID analyses. Samples were analyzed in full scan mode but quantified on extracted-ion GC–MS traces (*m/z* 178 and 192 for phenanthrene and methylphenanthrenes) with corrections for the relative response factor of each compound calculated from comparison of GC–FID with GC–MS ion traces on selected samples.

We use standard maturity indices to interpret the measured biomarker compositions. The best thermal maturity indicator present in the Punchbowl rocks was the methylphenanthrene index (Fig. 3). The methylphenanthrene index increases with thermal maturity as 9- and

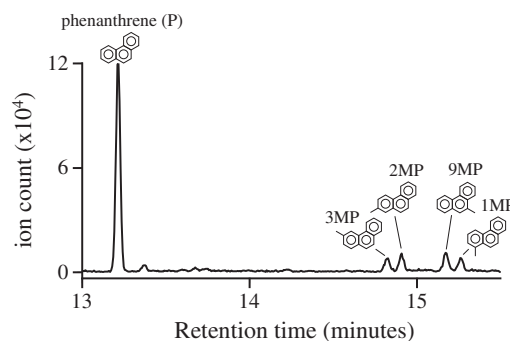


Fig. 3. A partial ion chromatogram of summed *m/z* 178 and 192 showing phenanthrene (P) and methylphenanthrenes (MP). The increased stability (lower steric strain) of phenanthrene and 3- and 2-methylphenanthrenes relative to 9- and 1-methylphenanthrenes is the basis for using these molecules as indicators of thermal maturity.

1-methylphenanthrenes become less abundant relative to the more thermally stable phenanthrene and 2- and 1-methylphenanthrenes.

The methylphenanthrene index (MPI 1) is calculated as:

$$\text{MPI1} = \frac{1.5(\text{MP3} + \text{MP2})}{\text{P} + \text{MP9} + \text{MP1}} \quad (6)$$

As discussed above, there are currently no measurements for the kinetics of the methylphenanthrene index. However, MPI 1 has been correlated to vitrinite reflectance, whose kinetics have been investigated. Therefore in order to quantitatively investigate the effects of heating on our samples we inferred the equivalent vitrinite reflectance from the MPI 1 values using the low-maturity equation of Radke (1988):

$$R_0 = 0.6\text{MPI1} + 0.4 \quad (7)$$

Throughout this paper, the values of R_0 based on measurements of MPI 1 and Eq. (7) are referred to as “inferred vitrinite reflectance” to distinguish them from direct measurements of vitrinite. By using Eq. (4) with the inferred vitrinite reflectances, we arrive at estimates of the thermal history.

4. Results from biomarker analysis and implications for heating along the Punchbowl Fault

4.1. Thermal maturity analysis

We find no heating difference between fault and off-fault rocks, based on the scatter of the vitrinite values inferred from the methylphenanthrenes. The inferred vitrinite values are 0.50–0.68 for the Punchbowl gouge and 0.60–0.73 for the off-fault rocks, including one sample that was approximately 15 m off the fault (Table 1, Fig. 4). The mean values of the on- and off-fault rocks are within two standard deviations of each other, indicating no differential heating. These values are consistent with vitrinite values inferred from alternative methylphenanthrene-based indices such as the PP-1 and MPR (Table 1, Alexander et al., 1986; Radke et al., 1986; Szczerba and Rospondek, 2010). Maturity ratios from other polycyclic aromatic hydrocarbons (phenylanthracenes, terphenyls and phenylphenanthrenes) also indicate no differential heating of fault and off-fault rocks (Table 1, Marynowski et al., 2001; Rospondek et al., 2009). Sterane and hopane maturity parameters (sterane C₂₀ and hopane C₂₂ S/[S+R]) have reached their maximum values, consistent with the geologic constraints on the amount of burial heating. Slow burial heating rather than rapid frictional heating is also suggested by the sterane and hopane values because, according to current knowledge of their reaction kinetics, these indices reach their maximum values before methylphenanthrenes

Table 1

Geochemical results from Punchbowl locality. The MPI 1 is defined in the text, $PP-1 = 1-MP/(2-MP + 3-MP)$ (Alexander et al., 1986; Szczerba and Rospondek, 2010) and decreases with increasing maturity, $MPR = 2-MP/1-MP$ (Radke et al., 1986; Szczerba and Rospondek, 2010), phenylanthracene ratio = 2-phenylanthracene/1-phenylanthracene (Marynowski et al., 2001), terphenyl ratio = p -terphenyl/ o -terphenyl (Marynowski et al., 2001), and the phenylphenanthrene ratio = $(2- + 3-PhP)/(2- + 3- + 4- + 1- + 9-PhP)$ (Rospondek et al., 2009).

# ^a	Location	MPI 1 ^b	R_0 from MPI 1 ^b	PP-1 ^b	MPR ^b	Phenylanthracene ratio ^{c,d}	Terphenyl ratio 1 ^{c,d}	Phenylphenanthrene ratio ^c
PB112809-01	Gouge	0.33	0.60	0.83	0.72	4.4	1.5	0.67
PB112809-02	Gouge	0.17	0.50	0.63	0.97	3.4	1.5	0.78
PB112809-03	>1 m from fault	0.41	0.65	0.58	1.11	2.5	1.3	0.68
PB112809-06	Gouge	0.46	0.68	0.41	1.75	n.d. ^e	1.9	n.d. ^e
PB112809-07	>1 m from fault	0.43	0.66	0.40	1.79	1.8	0.8	0.68
PB112809-09	Gouge	0.25	0.55	0.52	1.26	2.9	2.9	0.83
PB112809-10	>1 m from fault	0.51	0.71	0.36	1.94	1.4	1.1	0.69
PB112809-11	Gouge	0.30	0.58	0.56	1.15	2.8	2.6	0.83
PB112809-12	Gouge	0.23	0.54	0.56	1.24	3.5	2.3	0.83
PB112809-13	15 m from fault	0.55	0.73	0.58	1.18	2.4	1.5	0.54
SF112809-01		1.27	1.16	0.16	4.46	74.7	82.4	0.94
SF112809-02		1.23	1.14	0.16	4.61	66.1	37.1	0.93
Averages ($\pm 1\sigma$)	Gouge	0.29 ± 0.10	0.57 ± 0.06	0.58 ± 0.14	1.18 ± 0.34	3.4 ± 0.7	2.1 ± 0.6	0.79 ± 0.07
	>1 m from fault	0.45 ± 0.05	0.67 ± 0.03	0.45 ± 0.11	1.61 ± 0.44	1.9 ± 0.6	1.1 ± 0.3	0.68 ± 0.01
	15 m	0.55	0.73	0.58	1.18	2.4	1.5	0.54
	San Francisquito	1.25 ± 0.03	1.15 ± 0.02	0.16 ± 0.00	4.54 ± 0.11	70.4 ± 6.1	59.7 ± 32.0	0.94 ± 0.01

^a Prefix indicates Punchbowl (PB) or San Francisquito (SF) Formations.

^b Values calculated from GC–MSD ion traces corrected for response factors.

^c Values calculated from GC–MSD ion traces uncorrected for response factors.

^d Log of ratio is proportional to vitrinite reflectance.

^e Not detected.

when heating is slow (Elie and Mazurek, 2008; Mackenzie and McKenzie, 1983; Marzi et al., 1990; Sweeney and Burnham, 1990). However, this is a qualitative assessment based on the relationship of these other maturity parameters to methylphenanthrenes, the kinetics of these parameters have not been quantitatively evaluated.

It is important to note that the molecules we extracted from the samples are derived from organic matter within these rocks and therefore reflect the *in situ* time–temperature history. Petroleum and its precursors can potentially be highly mobile and pond against faults. There are five separate lines of evidence that such migration did not occur in the case of the Punchbowl samples: (i) the thermal maturity of the measured organics is what is expected from burial, (ii) the very low concentration of extractable organic matter in the rocks is less than would be present from petroleum migration, (iii) the basement rocks on the opposite side of the fault have no extractable organic material, as expected for rocks of their metamorphic grade, (iv) the most likely petroleum source, marine shales of the Paleocene San Francisquito formation, has a very different biomarker signature from the Punchbowl Fault samples (based upon our own analyses of San Francisquito rocks, Table 1), and (v) in a different site discussed below we can identify several of the above features when hydrocarbon migration has occurred.

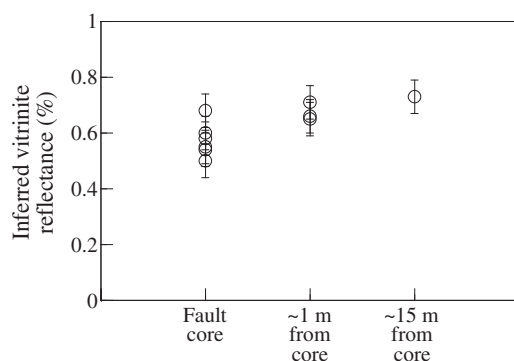


Fig. 4. Inferred vitrinite reflectance of Punchbowl Fault rocks from the methylphenanthrene index (MPI 1). No differential heating is seen between the fault and off-fault rocks.

There are three key observations in the geochemical data: (1) the samples from both the gouge and damage zone have the same thermal maturity, meaning that there was no differential heating on and off-fault, (2) the phenanthrenes and other polycyclic aromatic hydrocarbons present after the total slip history provide a temperature estimate that is consistent with burial heating and (3) the presence of 9-methylphenanthrene constrains the maximum temperature experienced by the samples to less than ~ 800 °C for a 1.5 s duration of heating (based upon extrapolation of laboratory kinetics, Behar et al., 1999). Given the analytical uncertainty ($\sim \pm 0.01\%$ R_0) and the natural variability of the Punchbowl samples, it would be difficult to detect less than a 0.2% vitrinite anomaly. This value is a conservative estimate based upon the 99% confidence interval calculated from the gouge and off fault rocks ($\sigma = 0.08$). From this uncertainty, we can calculate the upper bound for the maximum temperature above burial that the rocks could have experienced. Assuming timescales on the order of 10 s for an earthquake, the temperature rise above background did not exceed $\Delta T = \sim 400$ °C (this excess time–temperature would increase the phenanthrene maturity beyond the between-sample variability). Another upper temperature bound for the samples is provided by reaction kinetics determined from laboratory pyrolysis experiments on 9-methylphenanthrene (Behar et al., 1999). These experiments indicate that nearly complete destruction (99.9%) of this molecule would occur during 1.5 s of heating at $\Delta T = \sim 700$ °C.

4.2. Constraints on burial, friction, total slip and slip zone thickness

We will now proceed to interpret the data in terms of a simple physical model for burial and faulting (Lachenbruch, 1986) coupled to the kinetics of vitrinite maturation (Sweeney and Burnham, 1990).

The Punchbowl Fault has been proposed to have been active for 1–4 My at a depth of 2–4 km. The Punchbowl Formation most likely formed as sedimentary deposits in a pull-apart basin that initiated in the Middle Miocene (Chester and Chester, 1998), so burial time of the rocks could have been up to 12 My. Based on our results here and a range of geothermal gradients from 20 to 30 °C/km, we can limit the burial depth between 3 and 4 km, refining the sedimentary constraints (Fig. 5).

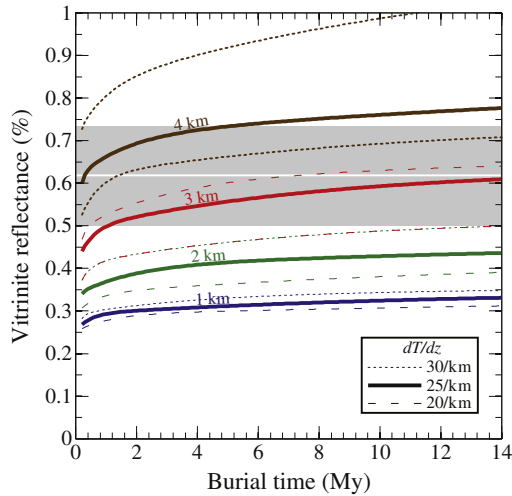


Fig. 5. Effects of burial depth and time on vitrinite reflectance with a surface temperature of 20 °C and geothermal gradients of 20, 25 and 30 °C/km. Shaded area bounds the range of inferred vitrinite values measured on Punchbowl rocks and the white line is the mean.

The temperature rise during a slip event can be computed by balancing the heat dissipated by friction and the temperature increase in the fault core (Lachenbruch, 1986),

$$\Delta T = \frac{\mu(1-\lambda)\sigma_n D}{\rho h c_p} = \frac{\mu(1-\lambda)gdD}{hc_p} \quad (8)$$

where ΔT is the temperature increase over the preseismic temperature, c_p is the specific heat capacity, h is the thickness of the slipping zone, ρ is the density of the rock, d is the depth of fault slip, μ the coefficient of friction, λ is the ratio of pore fluid pressure to overburden (taken as the density ratio of water/rock), σ_n is the normal stress and D is the slip in an event (Table 2 lists values). Eq. (8) gives a maximum value for temperature rise for a slip averaged friction value; we do not explicitly include complications such as slip and time dependent friction due to weakening mechanisms like thermal pressurization, as well as more complicated time histories of velocity (Andrews, 2005; Bizzarri and Cocco, 2006a, 2006b). For the Punchbowl example, we use the overburden ρgh for the normal stress on the strike-slip fault (second half of Eq. 8). Depth of faulting on the Punchbowl is estimated between 2 and 4 km (Chester and Logan, 1986) and for the purposes of this calculation, we use 3 km. The Punchbowl Fault is thought to have been active for 1–4 Ma. Here we consider the activity to take place over 3 Ma. We approximate the temperature history as a series of boxcar temperature rises equally spaced in time over the burial history. As a first-order approximation, we set the slip velocity to 1 m/s, so the time of heating for the events described here vary from fractions to tens of seconds.

The upper bound of $\Delta R_0 = 0.2\%$ derived from the organic measurements and Eq. (8) provide a constraint on a combination of the

Table 2
Parameters used in fault modeling.

Parameter	Description	Value	Reference
μ	Thermal diffusivity	$0.01 \text{ cm}^2 \text{ s}^{-1}$	(Lachenbruch, 1986)
c_p	Heat capacity	$1 \text{ kJ kg}^{-1} \text{ K}^{-1}$	(Lachenbruch, 1986)
D_{tot}	Total fault displacement	44 km	(Schulz and Evans, 2000)
d	Depth	3 km (range from sediment thickness is 2–4 km)	(Chester and Logan, 1986)
σ_n	Normal stress on fault	Overburden (ρgd)	
v	Slip velocity	1 m s^{-1}	(Kanamori and Brodsky, 2004)

coefficient of friction, slip and slip zone thickness (Fig. 6). We find that for a fault zone thickness of 1 mm as previously proposed (Chester and Chester, 1998), any reasonable value of the coefficient of friction (≥ 0.1) results in a maximum allowable slip during any event of <13 cm. Furthermore, only one event of this size could have occurred, or else the extra heating would have caused a detectable thermal anomaly. If the fault is as highly localized as previous work suggests, then our results allow us to estimate a maximum earthquake magnitude. By using the inferred maximum slip and assuming a stress drop between 0.3 and 10 MPa, we can combine the equations for seismic moment and stress drop (Kanamori and Anderson, 1975):

$$M_0 = \left(\frac{C}{\Delta\sigma}\right)^2 (GD)^3 \quad (9)$$

where $\Delta\sigma$ is stress drop, G is shear modulus and C is a shape factor equal to $\pi/2$ on a strike slip fault. From seismic moment, we can convert to moment magnitude (Hanks and Kanamori, 1979). Our results imply that the Punchbowl Fault never had an earthquake of magnitude greater than 6, assuming a 1 mm thick fault. The full parameter space is explored in Fig. 6. Given typical maximum earthquake-fault length scalings, we think that such a small maximum magnitude for the ~40 km long Punchbowl Fault is unlikely. However, it cannot be strictly ruled out by the data here (Table 3).

In addition, we calculate heating for a continually creeping fault for 44 km over 4 Ma. We use 4 Ma in this scenario because it represents the least heating (slowest velocity) that satisfies the geologic limitations. In this scenario the length of the slip event is longer than the dissipation time of heat from diffusion and we therefore model the temperature rise from a continuous source using the diffusive thickness as the effective width (Lachenbruch, 1986),

$$\Delta T = \frac{2\mu(1-\lambda)\rho g d v \sqrt{t}}{\rho c_p \sqrt{\pi\alpha}} \quad (10)$$

where α is thermal diffusivity, t is time, and v is slip velocity. For a creeping fault, we assume v is the value of total displacement (44 km)

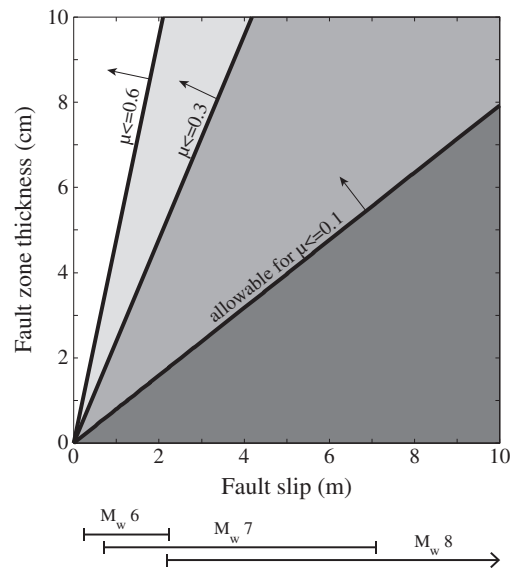


Fig. 6. Constraints on fault slip, thickness, and friction given the lack of heating signature above burial at the Punchbowl Fault. The areas above the lines of friction on the plot represent the parameter space that is allowable if the fault had that slip-averaged frictional strength. For instance, the white area in the upper left of the plot contains acceptable values of thickness and fault slip combinations that would not produce a heating signature above burial temperatures if the fault had a frictional strength of 0.6 or less. The fault slip and thickness values below the 0.6 line would produce more temperature rise than allowed by the data. Modeling assumed a depth of 3 km during faulting.

divided by time of active faulting (4 My). Given a burial depth of 3 km and hydrostatic pore pressure, we find that if the fault was creeping continuously, the coefficient of friction along the fault was less than 0.14. This solution for an infinitesimally thin fault is an upper bound on the heating expected for a given shear and can be mitigated by more distributed shear as discussed below. Additionally, if shorter time-scales (e.g. 1 Ma of active faulting) are used the predicted frictional heat increase would be even greater than what we calculated for 4 Ma because the temperature rise is linearly related to velocity while only related to the square root of time (Eq. 9).

4.3. Implications for fault processes

The modeling constraints on friction, slip distance and fault zone width suggest certain material properties and processes that may have been active along the Punchbowl during earthquakes. First, if the active shear zone was as localized as previously suggested, coseismic friction would need to have been very low or the effective stress was low. The coefficient of friction in active strands at the SAFOD drill core is ~0.1–0.2 (Carpenter et al., 2011), which although much lower than values predicted by Byerlee's law, would still be too strong to explain the lack of heat anomaly at Punchbowl for earthquakes with slip greater than 5–12 cm on a 1 mm slip surface. Although high velocity friction experiments have shown that gouge can be significantly weaker at earthquake slip speeds, these experiments seldom show dynamic friction values below 0.1 (Di Toro et al., 2011) except for extremely large displacements or in carbonate lithologies (e.g. Han et al., 2007; Mizoguchi et al., 2009).

One suggested mechanism to sustain low effective pressure during earthquakes is thermal pressurization due to heat generated from slip (Bizzarri and Cocco, 2006a, 2006b; Rempel and Rice, 2006; Rice, 2006). For thin fault zones where the hydraulic diffusivity approximately equals the thermal diffusivity, the temperature rise needed to pressurize the fault is below our detection threshold and thus could have contributed to a lower effective pressure on the Punchbowl Fault. However, for highly damaged rock such as those found around faults, the hydraulic diffusivity is most likely 10^{-4} – 10^{-5} m²/s, which is much greater than the thermal diffusivity (Doan et al., 2006). Rempel and Rice (2006) show that in this scenario, temperature rise can be very large (>1000 °C) for even moderate size earthquakes within the depths we are considering here. Because the rocks surrounding the Punchbowl Fault are extremely damaged, mechanisms beyond thermal pressurization should be explored to explain the lack of heating signature.

Our primary results constrain the peak temperature in the fault zone before transport of energy out of the fault core. Later advection of fluid could spread hot fault fluid outside the core resulting in elevated temperatures over a broad region. Many studies attempting to directly measure the temperature in the fault zone have been concerned with this possible advective effect (e.g., Fulton et al., 2010). However, later advection only decreases the temperature in the core after the peak reactions have already occurred. Therefore, advection does not explain the low values of peak temperature inferred here or the consistency of the temperature with the burial history.

Although we cannot rule out that the processes or material properties outlined above (low effective stress, low coefficient of friction, advected heat, smaller earthquakes) occurred over the lifetime of the Punchbowl Fault, we prefer the explanation that larger earthquakes occurred over thicknesses greater than 1 mm. Given the mapped surface trace of the fault and its previous continuity with the now-active strand, we would expect the largest rupture length to be approximately M8 (Wells and Coppersmith, 1994). The entire ultracataclastic zone at Punchbowl is 4–10 cm thick. If this entire thickness was active during shearing, extremely large earthquakes could have been hosted along the Punchbowl without a significant contribution to frictional heat.

Table 3

Geochemical results from the Sitkalidak Formation, Kodiak Accretionary Complex.

#	Location	MPI 1	R ₀ from MPI 1 ^a	R ₀ measured ^b
CL-020713-12 ^c	Inside shear zone	0.31 ± 0.01	0.59 ± 0.01	–
Sk5b	Inside shear zone	0.40	0.64	0.60
Sk21B	Inside shear zone	0.26	0.55	0.65
Sk6c	Outside shear zone	0.50	0.70	0.61
Sk11a	Outside shear zone	0.43	0.66	0.51
Sk28h	Outside shear zone	0.49	0.70	0.56
Averages	Inside shear zone	0.32 ± 0.07	0.59 ± 0.04	0.63 ± 0.04
(± 1σ)	Outside shear zone	0.48 ± 0.04	0.69 ± 0.03	0.56 ± 0.05

^a Values calculated from GC–MSD ion traces corrected for response factors.

^b Vitrinite reflectance values from Moore and Allwardt (1980).

^c Average of six subsamples from a 10 × 2 × 1 cm hand sample.

5. Results of biomarker analysis in other fault zones

Here we describe results from two other fault zones that were more difficult to interpret than the results at the Punchbowl Fault. In the case of the small faults in the Santa Cruz region, migrated petroleum swamped any *in situ* organics that could be measured. The results for the Kodiak Accretionary Complex are more complicated, and discussed in detail below.

5.1. Santa Cruz region, California

Samples of fault gouge and adjacent rocks from a series of small faults in the Santa Cruz mudstone (local upper member of the Monterey formation, diatomaceous mudstone) were analyzed. Three of the faults were from Four Mile Beach (Savage and Brodsky, 2011) and occur in the lower part of the Santa Cruz mudstone while the fourth fault is in the upper part of the Santa Cruz mudstone at Natural Bridges State Park, Santa Cruz. The faults from the lower Santa Cruz Fm. contained large amounts of extractable bitumen and in most cases, tarry deposits coat fracture surfaces and are pervasive in the fault gouge.

We found no maturity difference between gouge and host rocks for any of the four faults. The presence of bitumen in fractures indicates expulsion and migration has occurred, meaning the material extracted from these rocks is not necessarily derived from the rocks we sampled. The Santa Cruz mudstone itself could be a source, as could the deeper Monterey Formation. The intervening, discontinuous Santa Margarita Sandstone that separates the Monterey from Santa Cruz mudstone is also a potential reservoir and migration pathway for fluids from thicker, more deeply buried Monterey and Santa Cruz mudstone rocks to the north (see Boehm and Moore, 2002 for a cross section). The thermal maturity indicators in these bitumens are consistent with a Monterey-type source, with mature hopane C₂₂ S/[S + R] ratios but relatively immature sterane C₂₀ S/[S + R] and [17α + 21α]/[17α + 21α + 17β + 21β] ratios. Triterpenoid and other biomarkers are also similar to Monterey-type

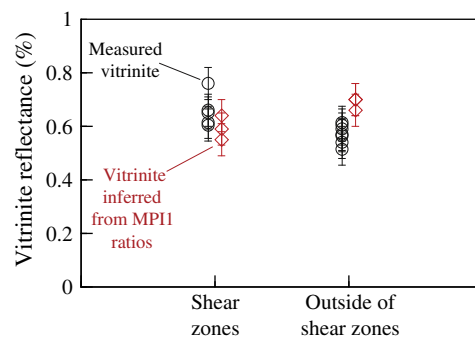


Fig. 7. Vitrinite reflectance values and inferred vitrinite reflectance (from MPI 1 values) for the Sitkalidak rocks. Vitrinite reflectance data is from Moore and Allwardt (1980).

oils (c.f. Hostettler et al., 2004). As faulting could post-date petroleum migration, the lack of differential heating of the faults could be consistent with the small offsets and relatively shallow burial depths. However, it is more likely that migration occurred syn- or post-faulting and that the similar maturity ratios simply reflect that of the petroleum source rocks.

5.2. Kodiak Accretionary Complex, Alaska

We measure thermal maturity on mudstones from the Sitkalidak Fm. on Sitkanik Island, in the Kodiak archipelago, Alaska (Moore and Allwardt, 1980; Rowe, 2007). The rocks in the study area are part of the Kodiak Accretionary Complex. An important difference between this study area and the previous two is that there is no intact 'background' rock. The 'on-fault' samples represent rocks from km-scale shear zones that are potentially ancient megathrusts (Moore and Allwardt, 1980). The 'off-fault' samples are taken from outside of these extremely large shear zones, but are still highly faulted and folded mélangé rocks. The complicated burial history of the area makes simple time–temperature modeling of burial difficult (Moore and Allwardt, 1980), however the estimated burial depth was approximately 3 km.

Moore and Allwardt (1980) investigated burial and heating of these rocks by measuring porosity and vitrinite reflectance. We analyze a subset of the samples used in Moore and Allwardt (1980), focusing only on the mélangé samples that the authors referred to as 'more deformed Sitkalidak Fm.' and regroup the original samples into shear zone and non-shear zone samples. An additional shear zone sample was measured as well (Rowe, 2007). Previously measured vitrinite reflectance from these rocks indicate a modest increase of the reflectance values in shear zone rocks compared to those outside of shear zones (Fig. 7). From the same samples of the original study, inferred vitrinite values from MPI 1 ratios outside the shear zones are slightly higher than the range of the measured vitrinite. Within the shear zone the vitrinite values inferred from the MPI ratios are indistinguishable from the measured values (Fig. 7). These differences are small and could merely reflect that not enough samples were analyzed to reflect the true variability. However, we cannot rule out that this is a migrated petroleum signal. Additional analyses are needed to determine whether the extractable bitumen is indigenous and reflects local conditions or is migrated and part of a larger-scale petroleum system.

6. Limitations, uncertainties and directions for future research

Fault zones are among the most effective traps for migrating hydrocarbons. Therefore, the greatest challenge in site selection is to find a fault with sufficient *in situ* organics to be resolvable while being free of contaminating hydrocarbons that may have migrated from off-fault. The Punchbowl Fault satisfies these criteria as it is embedded in a coarse-grained terrestrial sedimentary unit with extremely low concentrations of organics, much less than expected if there had been migration of petroleum. In the Santa Cruz faults, migration of hydrocarbons obscures the fault zone signature. The Kodiak Accretionary Complex is the most structurally complicated fault system studied here and requires additional analysis before any conclusive heating estimate could be made. We present these unique data here both for their value for fault mechanics and to illustrate some of the potential difficulties when working with bitumen biomarkers in fault zones.

The influence of fluid advection on the thermal regime in fault zones is a potentially confounding factor in any study of fault heating. Because thermal maturation is irreversible and strongly sensitive to peak temperatures, it is potentially less sensitive to advection compared to integrated measures of heating such as direct measurement of borehole temperatures. While not a focus of this paper, inclusion of

fault hydrology when modeling thermal maturation in fault zones could provide additional constraints on fault processes.

Finally, another source of uncertainty is our limited understanding of biomarker kinetics at fast heating rates, as discussed in Section 2. Future work should focus on determining maturation kinetics of biomarkers and vitrinite at earthquake heating rates in order to quantitatively constrain maximum temperatures. Fortunately, such heating rates are readily accessible in the lab.

7. Conclusions

We present a new paleothermometer using the thermal maturity of organic matter to detect heating in exhumed faults. This technique allows for temperature estimates on the many fault zones hosted in sedimentary rock, and does not need to be limited to exhumed faults. Our analysis of the Punchbowl Fault, southern California, shows no additional heating above background, indicating that frictional heating from fault slip was low. Furthermore, this technique successfully limited the potential burial range to 3–4 km. To achieve minimal frictional heating over 44 km of displacement, the Punchbowl Fault must have 1) had a low coefficient of friction (~0.1), 2) had low effective stress, 3) slipped in small earthquakes, and/or 4) had an active slipping surfaces thicker than 1 mm. Results from other faults in our study show more ambiguous results, possibly related to the migration of hydrocarbons. This work represents a promising new avenue in detecting heat signatures along faults.

Acknowledgments

We would like to thank Nicholas van der Elst for help collecting samples, Elena Amador for assistance with sample preparation, Casey Moore for donating samples from Alaska and guiding the regrouping of on- and off-fault samples, Christie Rowe for donating samples from Alaska and insightful comments on early manuscripts, and Matt McCarthy for generous use of his GC–MS. Fred Chester and an anonymous reviewer provided insightful suggestions to improve this paper. This work was supported by NSF-EAR 0948740.

References

- Alexander, R., Strachan, M.G., Kagi, R.I., Van Bronswijk, W., 1986. Heating rate effects on aromatic maturity indicators. *Org. Geochem.* 10, 997–1003.
- Alexander, R., Kralert, P.G., Kagi, R.I., 1992. Kinetics and mechanism of the thermal decomposition of esters in sediments. *Org. Geochem.* 19, 133–140.
- Alexander, R., Kralert, P.G., Sosrowidjojo, I.B., Kagi, R.I., 1997. Kinetics and mechanism of the thermal elimination of alkenes from secondary stanyl and triterpenyl esters: implications for sedimentary processes. *Org. Geochem.* 26, 391–398.
- Andrews, D.J., 2005. Rupture dynamics with energy loss outside the slip zone. *J. Geophys. Res.* 110 (B1), B01307.
- Beaumont, C., Boutilier, R., Mackenzie, A.S., Rullkotter, J., 1985. Isomerization and aromatization of hydrocarbons and the paleothermometry and burial history of Alberta Foreland Basin. *AAPG Bull.* 69 (4), 546–566.
- Behar, F., Budzinski, H., Vandenbroucke, M., Tang, Y., 1999. Methane generation from oil cracking: kinetics of 9-methylphenanthrene cracking and comparison with other pure compounds and oil fractions. *Energy Fuels* 13, 471–481. 10.1021/ef980164p.
- Bishop, A.N., Abbott, G.D., 1995. Vitrinite reflectance and molecular geochemistry of Jurassic sediments: the influence of heating by Tertiary dykes (northwest Scotland). *Org. Geochem.* 22 (1), 165–177.
- Bizzarri, A., Cocco, M., 2006a. A thermal pressurization model for the spontaneous dynamic rupture propagation on a three-dimensional fault: 1. Methodological approach. *J. Geophys. Res.* 111 (B5), B05303.
- Bizzarri, A., Cocco, M., 2006b. A thermal pressurization model for the spontaneous dynamic rupture propagation on a three-dimensional fault: 2. Traction evolution and dynamic parameters. *J. Geophys. Res.* 111 (B5), B05304.
- Boehm, A., Moore, J.C., 2002. Fluidized sandstone intrusions as an indicator of Paleostress orientation, Santa Cruz, California. *Geofluids* 2 (2), 147–161.
- Bowden, S.A., Court, R.W., Milner, D., Baldwin, E.C., Lindgren, P., Crawford, I.A., Parnell, J., Burchell, M.J., 2008. The thermal alteration by pyrolysis of the organic component of small projectiles of mudrock during capture at hypervelocity. *J. Anal. Appl. Pyrolysis* 82 (2), 312–314.
- Bowden, S.A., Parnell, J., Burchell, M.J., 2009. Survival of organic compounds in ejecta from hypervelocity impacts on ice. *Int. J. Astrobiol.* 8, 19–25 (Special Issue 01).

- Brune, J.N., Henyey, T.L., Roy, R.F., 1969. Heat flow, stress, and rate of slip along the San Andreas Fault, California. *J. Geophys. Res.* 74 (15), 3821–3827.
- Burnham, A.K., Braun, R.L., 1998. Global kinetic analysis of complex materials. *Energy Fuels* 13 (1), 1–22.
- Burnham, A.K., Sweeney, J.J., 1989. A chemical kinetic model of vitrinite maturation and reflectance. *Geochim. Cosmochim. Acta* 53 (10), 2649–2657.
- Bustin, R.M., 1983. Heating during thrust faulting in the rocky mountains: friction or fiction? *Tectonophysics* 95 (3–4), 309–328.
- Carpenter, B.M., Marone, C., Saffer, D.M., 2011. Weakness of the San Andreas Fault revealed by samples from the active fault zone. *Nat. Geosci.* 4 (4), 251–254.
- Chester, F.M., Chester, J.S., 1998. Ultracataclastic structure and friction processes of the San Andreas fault. *Tectonophysics* 295, 199–221.
- Chester, F.M., Logan, J.M., 1986. Implications for mechanical properties of brittle faults from observations of the Punchbowl Fault Zone, California. *Pure Appl. Geophys.* 124 (1/2), 79–106.
- Chester, F.M., Evans, J., Biegel, R.L., 1993. Internal structure and weakening mechanisms of the San Andreas fault. *J. Geophys. Res.* 98 (B1), 771–786.
- d'Alessio, M.A., Blythe, A.E., Burgmann, R., 2003. No frictional heat along the San Gabriel fault, California: evidence from fission-track thermochronology. *Geology* 31 (6), 541–544.
- Daly, T.K., Buseck, P.R., Williams, P., Lewis, C.F., 1993. Fullerenes from a fulgurite. *Science* 259 (5101), 1599–1601.
- Di Toro, G., Han, R., Hirose, T., De Paola, N., Nielsen, S., Mizoguchi, K., Ferri, F., Cocco, M., Shimamoto, T., 2011. Fault lubrication during earthquakes. *Nature* 471 (7339), 494–498.
- Doan, M.L., Brodsky, E.E., Kano, Y., Ma, K.F., 2006. In situ measurement of the hydraulic diffusivity of the active Chelungpu Fault, Taiwan. *Geophys. Res. Lett.* 33 (16), L16317. doi:10.1029/2006GL026889.
- Dor, O., Rockwell, T., Ben-Zion, Y., 2006. Geological observations of damage asymmetry in the structure of the San Jacinto, San Andreas and Punchbowl Faults in Southern California: a possible indicator for preferred rupture propagation direction. *Pure Appl. Geophys.* 163 (2), 301–349.
- Elie, M., Mazurek, M., 2008. Biomarker transformations as constraints for the depositional environment and for maximum temperatures during burial of Opalinus Clay and Posidonia Shale in northern Switzerland. *Appl. Geochem.* 23 (12), 3337–3354. doi:10.1016/j.apgeochem.2008.3305.3022.
- Farrimond, P., Bevan, J.C., Bishop, A.N., 1999. Tricyclic terpane maturity parameters: response to heating by an igneous intrusion. *Org. Geochem.* 30 (8, Part 2), 1011–1019.
- Fulton, P.M., Harris, R.N., Saffer, D.M., Brodsky, E.E., 2010. Does hydrologic circulation mask frictional heat on faults after large earthquakes? *J. Geophys. Res.* 115 (B9), B09402.
- Han, R., Shimamoto, T., Hirose, T., Ree, J.-H., Ando, J.-i., 2007. Ultralow friction of carbonate faults caused by thermal decomposition. *Science* 316, 878–881.
- Hanks, T.C., Kanamori, H., 1979. A moment magnitude scale. *J. Geophys. Res.* 84 (B5), 2348–2350.
- Hostettler, F.D., Rosenbauer, R.J., Lorenson, T.D., Dougherty, J., 2004. Geochemical characterization of tarballs on beaches along the California coast. Part I—shallow seepage impacting the Santa Barbara Channel Islands, Santa Cruz, Santa Rosa and San Miguel. *Org. Geochem.* 35, 725–746. doi:10.1016/j.orggeochem.2004.01.022.
- Kanamori, H., Anderson, D.L., 1975. Theoretical basis for some empirical relations in seismology. *Bull. Seismol. Soc. Am.* 65, 1073–1095.
- Kanamori, H., Brodsky, E.E., 2004. The physics of earthquakes. *Rep. Prog. Phys.* 67, 1429–1496. doi:10.1088/0034-4885/1467/1428/R1403.
- Kano, Y., Mori, J., Fujio, R., Ito, H., Yanagidani, T., Nakao, S., Ma, K.-F., 2006. Heat signature on the Chelungpu fault associated with the 1999 Chi-Chi, Taiwan earthquake. *Geophys. Res. Lett.* 33 (14), L14306.
- Kirkpatrick, J.D., Shipton, Z.K., Persano, C., 2009. Pseudotachylites: rarely generated, rarely preserved or rarely reported? *Bull. Seismol. Soc. Am.* 99, 382–388. doi:10.1785/0120080114.
- Lachenbruch, A.H., 1986. Simple models for the estimation and measurement of frictional heating by an earthquake. United States Geological Survey Open-File Report 86–508, 13.
- Lachenbruch, A.H., Sass, J.H., 1980. Heat flow and energetics of the San Andreas Fault Zone. *J. Geophys. Res.* 85 (B11), 6185–6222.
- Lachenbruch, A.H., Sass, J.H., 1992. Heat flow from Cajon Pass: fault strength, and tectonic implications. *J. Geophys. Res.* 97 (B4), 4995–5015.
- Mackenzie, A.S., McKenzie, D., 1983. Isomerization and aromatization of hydrocarbons in sedimentary basins formed by extension. *Geol. Mag.* 120 (5), 417–470.
- Marynowski, L., Czechowski, F., Simoneit, B.R.T., 2001. Phenylanthracenes and polycyclic phenyls in Palaeozoic source rocks of the Holy Cross Mountains, Poland. *Org. Geochem.* 32 (1), 69–85.
- Marzi, R., Rullkötter, J., Perriman, W.S., 1990. Application of the change of sterane isomer ratios to the reconstruction of geothermal histories: implications of the results of hydrous pyrolysis experiments. *Org. Geochem.* 16 (1–3), 91.
- Mastalerz, M., Wilks, K.R., Bustin, R.M., Ross, J.V., 1993. The effect of temperature, pressure and strain on carbonization in high-volatile bituminous and anthracitic coals. *Org. Geochem.* 20 (2), 315–325.
- Mizoguchi, K., Hirose, T., Shimamoto, T., Fukuyama, E., 2009. High-velocity frictional behavior and microstructure evolution of fault gouge obtained from Nojima fault, southwest Japan. *Tectonophysics* 471 (3–4), 285–296. doi:10.1016/j.tecto.2009.02.033.
- Moore, J.C., Allwardt, A., 1980. Progressive deformation of a Tertiary trench slope, Kodiak Islands, Alaska. *J. Geophys. Res.* 85 (B9), 4741–4756.
- Mukoyoshi, H., Sakaguchi, A., Otsuki, K., Hirono, T., Soh, W., 2006. Co-seismic frictional melting along an out-of-sequence thrust in the Shimanto Accretionary Complex. Implications on the tsunamigenic potential of splay faults in modern subduction zones. *Earth Planet. Sci. Lett.* 245 (1–2), 330.
- O'Hara, K., 2004. Paleo-stress estimates on ancient seismogenic faults based upon frictional heating of coal. *Geophys. Res. Lett.* 31. doi:10.1029/2003GL018890.
- O'Hara, K., Hower, J.C., Rimmer, S.M., 1990. Constraints on the emplacement and uplift history of the Pine Mountain Thrust Sheet, Eastern Kentucky: evidence from coal rank trends. *J. Geol.* 98 (1), 43–51.
- O'Hara, K., Mizoguchi, K., Shimamoto, T., Hower, J.C., 2006. Experimental frictional heating of coal gouge at seismic slip rates: evidence for devolatilization and thermal pressurization of gouge fluids. *Tectonophysics* 424 (1–2), 109.
- Parnell, J., Bowden, S., Lindgren, P., Burchell, M., Milner, D., Price, M., Baldwin, E.C., Crawford, I.A., 2010. The preservation of fossil biomarkers during meteorite impact events: experimental evidence from biomarker-rich projectiles and target rocks. *Meteorit. Planet. Sci.* 45 (8), 1340–1358.
- Peters, K.E., Walters, C.C., Moldovan, J.M., 2004. *The Biomarker Guide*. Cambridge University Press, Cambridge, UK.
- Radke, M., 1988. Application of aromatic compounds as maturity indicators in source rocks and crude oils. *Mar. Pet. Geol.* 5 (3), 224.
- Radke, M., Welte, D.H., Willsch, H., 1986. Maturity parameters based on aromatic hydrocarbons: influence of the organic matter type. *Org. Geochem.* 10, 51–63.
- Raymond, A.C., Murchison, D.G., 1992. Effect of igneous activity on molecular-maturation indices in different types of organic matter. *Org. Geochem.* 18 (5), 725.
- Rempel, A.W., Rice, J.R., 2006. Thermal pressurization and onset of melting in fault zones. *J. Geophys. Res.* 111 (B9), B09314.
- Rice, J.R., 2006. Heating and weakening of faults during earthquake slip. *J. Geophys. Res.* 111 (B5), B05311.
- Rospondek, M.J., Marynowski, L., Chachaj, A., Góra, M., 2009. Novel aryl polycyclic aromatic hydrocarbons: phenylphenanthrene and phenylanthracene identification, occurrence and distribution in sedimentary rocks. *Org. Geochem.* 40 (9), 986–1004.
- Ross, J.V., Bustin, R.M., 1990. The role of strain energy in creep graphitization of anthracite. *Nature* 343 (6253), 58.
- Rowe, C.D., 2007. Snapshots of the earthquake cycle: An approach to subduction zone paleo-seismicity, Ph.D. dissertation, University of California, Santa Cruz.
- Rowe, C., Moore, J., Meneghini, F., McKiernan, A., 2005. Large-scale pseudotachylites and fluidized cataclases from an ancient subduction thrust fault. *Geology* 33 (12), 937–940.
- Sakaguchi, A., Yanagihara, A., Ujii, K., Tanaka, H., Kameyama, M., 2007. Thermal maturity of a fold-thrust belt based on vitrinite reflectance analysis in the Western Foothills complex, western Taiwan. *Tectonophysics* 443 (3–4), 220.
- Sakaguchi, A., Chester, F.M., Curewitz, D., Fabbri, O., Goldsby, D.L., Kimura, G., Li, C., Masaki, Y., Screenshot, E.J., Tsutsumi, A., Ujii, K., Yamaguchi, A., 2011. Seismic slip propagation to the updip end of plate boundary subduction interface faults: vitrinite reflectance geothermometry on Integrated Ocean Drilling Program NanTroSeize cores.
- Savage, H.M., Brodsky, E.E., 2011. Collateral damage: the evolution with displacement of fracture distribution and secondary fault strands in fault damage zones. *J. Geophys. Res.* 116, B03405. doi:10.1029/2010JB007665.
- Schimmelmann, A., Mastalerz, M., Gao, L., Sauer, P.E., Topalov, K., 2009. Dike intrusions into bituminous coal, Illinois Basin: H, C, N, O isotopic responses to rapid and brief heating. *Geochim. Cosmochim. Acta* 73 (20), 6264. doi:10.1016/j.gca.2009.07.027.
- Schulz, S.E., Evans, J., 2000. Mesoscopic structure of the Punchbowl Fault, Southern California and the geologic and geophysical structure of active strike-slip faults. *J. Struct. Geol.* 22, 913–930.
- Simoneit, B.R.T., 2002. Biomass burning – a review of organic tracers for smoke from incomplete combustion. *Appl. Geochem.* 17 (3), 129–162.
- Suchy, V., Frey, M., Wolf, M., 1997. Vitrinite reflectance and shear-induced graphitization in orogenic belts: a case study from the Kandersteg area, Helvetic Alps, Switzerland. *Int. J. Coal Geol.* 34 (1–2), 1.
- Sweeney, J.J., Burnham, A.K., 1990. Evaluation of a simple model of vitrinite reflectance based on chemical kinetics. *Am. Assoc. Pet. Geol. Bull.* 74 (10), 1559–1570.
- Szczerba, M., Rospondek, M.J., 2010. Controls on distributions of methylphenanthrenes in sedimentary rock extracts: critical evaluation of existing geochemical data from molecular modelling. *Org. Geochem.* 41, 1297–1311.
- Tanaka, H., Fujimoto, K., Ohtani, T., Ito, H., 2001. Structural and chemical characterization of shear zones in the freshly activated Nojima fault, Awaji Island, southwest Japan. *J. Geophys. Res.* 106 (B5), 8789–8810.
- Underwood, M.B., O'Leary, J.D., Strong, R.H., 1988. Contrasts in thermal maturity within terranes and across terrane boundaries of the Franciscan Complex, Northern California. *J. Geol.* 96 (4), 399–415.
- Wei, Z., Moldovan, J.M., Jarvie, D.M., Hill, R., 2006. The fate of diamondoids in coals and sedimentary rocks. *Geology* 34 (12), 1013–1016.
- Wells, D.L., Coppersmith, K.J., 1994. New empirical relationships among magnitude, rupture length, rupture width, rupture area, and surface displacement. *Bull. Seismol. Soc. Am.* 84, 974–1002.
- Wilks, K.R., Mastalerz, M., Bustin, R.M., Ross, J.V., 1993. The role of shear strain in the graphitization of a high-volatile bituminous and an anthracitic coal. *Int. J. Coal Geol.* 22 (3–4), 247–277.
- Wilson, J.E., Chester, J.S., Chester, F.M., 2003. Microfracture analysis of fault growth and wear processes, Punchbowl Fault, San Andreas system, California. *J. Struct. Geol.* 25, 1855–1873.